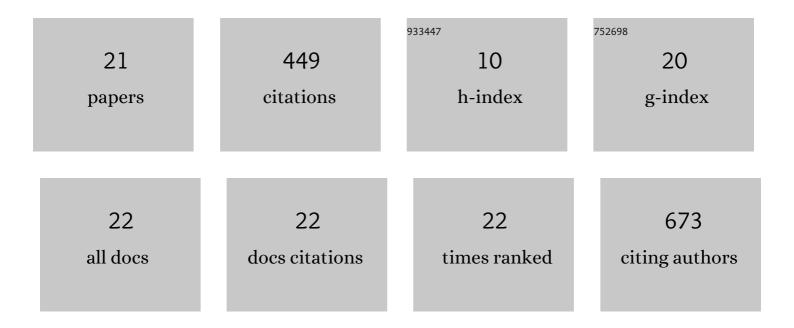
Misun Kang

List of Publications by Year in descending order

Source: https://exaly.com/author-pdf/3922291/publications.pdf Version: 2024-02-01



MISLIN KANC

#	Article	IF	CITATIONS
1	Neutron imaging of hydrogen-rich fluids in geomaterials and engineered porous media: A review. Earth-Science Reviews, 2014, 129, 120-135.	9.1	128
2	Water calibration measurements for neutron radiography: Application to water content quantification in porous media. Nuclear Instruments and Methods in Physics Research, Section A: Accelerators, Spectrometers, Detectors and Associated Equipment, 2013, 708, 24-31.	1.6	72
3	Neutron imaging reveals internal plant water dynamics. Plant and Soil, 2013, 366, 683-693.	3.7	45
4	Polymicrobial periodontal disease triggers a wide radius of effect and unique virome. Npj Biofilms and Microbiomes, 2020, 6, 10.	6.4	36
5	Diffusivity and Sorptivity of Berea Sandstone Determined using Neutron Radiography. Vadose Zone Journal, 2013, 12, 1-8.	2.2	26
6	Average Soil Water Retention Curves Measured by Neutron Radiography. Soil Science Society of America Journal, 2012, 76, 1184-1191.	2.2	25
7	Immunoproteomic Identification ofIn Vivo-Produced Propionibacterium acnes Proteins in a Rabbit Biofilm Infection Model. Vaccine Journal, 2015, 22, 467-476.	3.1	23
8	Multiple pixel-scale soil water retention curves quantified by neutron radiography. Advances in Water Resources, 2014, 65, 1-8.	3.8	21
9	Biomineralization of Dental Tissues Treated with Silver Diamine Fluoride. Journal of Dental Research, 2021, 100, 1099-1108.	5.2	17
10	Biomechanical pathways of dentoalveolar fibrous joints in health and disease. Periodontology 2000, 2020, 82, 238-256.	13.4	11
11	Architecture-Guided Fluid Flow Directs Renal Biomineralization. Scientific Reports, 2018, 8, 14157.	3.3	9
12	FoxO1 as a Regulator of Aquaporin 5 Expression in the Salivary Gland. Journal of Dental Research, 2021, 100, 1281-1288.	5.2	9
13	Microanatomical changes and biomolecular expression at the PDL â€entheses during experimental tooth movement. Journal of Periodontal Research, 2019, 54, 251-258.	2.7	8
14	Physicochemical and biochemical spatiotemporal maps of a mouse penis. Journal of Biomechanics, 2020, 101, 109637.	2.1	5
15	Structural and chemical heterogeneities of primary hyperoxaluria kidney stones from pediatric patients. Journal of Pediatric Urology, 2021, 17, 214.e1-214.e11.	1.1	3
16	Mineralized Peyronie's plaque has a phenotypic resemblance to bone. Acta Biomaterialia, 2022, 140, 457-466.	8.3	3
17	Evaluation of TrueCell program for estimating point capillary pressure — saturation parameters for Flint sand. Geoderma, 2017, 287, 90-97.	5.1	2
18	Data on biomechanics and elemental maps of dental implant-bone complexes in rats. Data in Brief, 2020, 31, 105969.	1.0	2

#	Article	IF	CITATIONS
19	Mechanoadaptive strain and functional osseointegration of dental implants in rats. Bone, 2020, 137, 115375.	2.9	2
20	Structure and elemental composition of Ceftriaxone induced pediatric nephrolithiasis. Urolithiasis, 2021, 49, 309-320.	2.0	2
21	Upscaling Capillary Pressure-Saturation Functions Using Different Reference Pressure Elevations. Vadose Zone Journal, 2017, 16, vzj2017.03.0054.	2.2	Ο